University of Padova

Department of Information Engineering

Master degree in Automation Engineering

Laboratory Report1: Position state–space control of a DC servomotor

Group 3, components: Davide Baron, Alessio Bonetto, Marco Mustacchi, Luca Vittorio Piron

Academic Year 2021-2022

1 Introduction

1.1 Activity Goal

This laboratory activity is articulated in two parts:
The first part reguards some improvements to the position PID–control system designed seen in the laboratory experience 0.
In particular, it has been introduced:

- The anti-windup mechanism, in order to reduce the large overshoot caused by the saturation of the controller output.
- A feedforward compensation for friction, inertia and BEMF, which allows to increase both the accuracy and speed of response respect to the conventional feedback control.

The second part of the experience is about the design of a continou-time position controller by using different state-space techniques. In the activity, both nominal and robust tracking designs are considered, in particular.

- The nominal tracking is performed using a conventional feedforwar scheme, adding a gain adjustment scheme.
- The robust tracking is implemented by either using an integral action (for robust trackin of constant set-points or perfect rejection of constant load disturbances), or by resorting to the internal model principle (for robust tracking and perfect rejection of more general, possibly time–varying signals), considering error-space and extended estimator approaches.

1.2 System and Model

The lumped-element diagram of the DC gearmotor is shown in Figure 1. All the symbols of the diagram are defined in the Figure 2. For the numerical values consult the Appendix A.

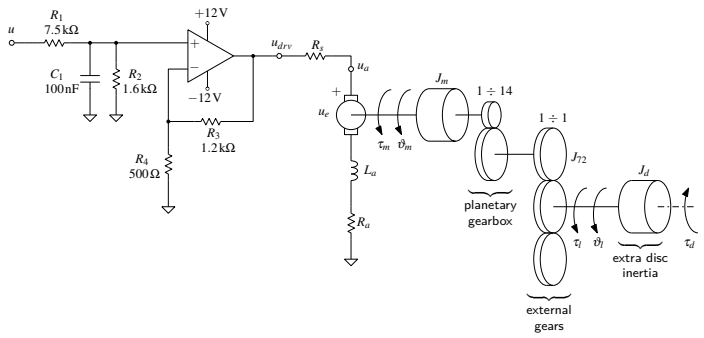

Figure 1: DC gearmotor: lumped-element diagram.

For our design process it is useful to compute the transfer function from the voltage driver

input u (that will be provided by the controller through a DAC) to the load angle θ_l, which will be provided by an optical encoder attached to the central shaft of the gearbox.

The model used to evaluate and perform the different control laws has been obtained as solution of ODE's relative to the motor, the driver and the geabox. The model of the DC gearmotor with inertal load is represented by the following ODE's:

$$\begin{cases} L_a \frac{di_a}{dt} + R_{eq} i_a & = u_{drv} - k_e \omega_m \\ J_{eq} \frac{d\omega_m}{dt} + B_{eq} \omega_m & = k_t i_a - \frac{1}{N} \tau_d \\ T_{drv} \frac{du_{drv}}{dt} + u_d rv & = k_{drv} u \end{cases} \tag{1}$$

By applying the Laplace transform it is possible to obtain the following transfer function:

$$P(s) = \frac{1}{sN} \cdot \frac{k_T}{(L_a s + R_{eq})(J_{eq} s + B_{eq}) + k_t k_e} \cdot \frac{k_{drv}}{1 + sT_{drv}} \tag{2}$$

This transfer function can be a bit simplified considering $La \ll R_{eq}$ and $T_{DRV} \ll 1$:

$$P(s) \simeq \frac{1}{sN} \cdot \frac{k_t k_{drv}}{R_{eq}(J_{eq} s + B_{eq}) + k_t k_e} = \frac{1}{sN} \cdot \frac{k_m}{1 + sT_m} \tag{3}$$

with:

$$k_m := \frac{k_{drv} k_t}{R_{eq} B_{eq} + k_t k_e} \quad T_m := \frac{R_{eq} J_{eq}}{R_{eq} B_{eq} + k_t k_e} \quad R_{eq} := R_a + R_s \tag{4}$$

The quantities:

$$B_{eq} = B_m + \frac{B_l}{N^2} = 1.2745 \cdot 10^{-6}\ Nms/rad$$
$$J_{eq} = J_m + \frac{J_l}{N^2} = 5.5567 \cdot 10^{-7}\ Nms^2/rad$$

were estimated in a previous laboratory activity together with the static friction value $\tau_s f = 0.0106$Nm. Such quantities were used in the building of the accurate Simulink model (also called "nominal model" in this report) of the DC servomotor (see the Appendix A).

J_m, B_m	rotor moment of inertia and viscous friction coefficient
J_l, B_l	load moment of inertia and viscous friction coefficient
R_a, L_a	resistance and inductance of the armature circuit
u_a, i_a	supply voltage and current to the armature circuit
u_e	back electromotive force (BEMF)
k_t, k_e	torque and electric (BEMF) constants
τ_m, ω_m, ϑ_m	*motor side* torque, speed and position
τ_l, ω_l, ϑ_l	*load side* torque, speed and position
τ_d	disturbance torque applied to the load inertia
N	planetary gearbox reduction ratio
R_s	shunt resistance
u, u_{drv}	voltage driver input and output voltages
k_{drv}, $f_{c,drv}$	voltage driver attenuation gain and cut–off frequency

Figure 2: DC gearmotor with inertial load: symbols definitions.

2 Tasks, Methodologies and Results

2.1 PID Controller

2.1.1 Anti-windup

When in the control loop an integrator component is present, the possibility of saturation of the control output occurs. This is principally due to the fact that the power supply is limited ad hence the controller is not able to provide whatever input voltage to the system.
This means that the controller is not applying what it wants, thus the system reacts more slowly than the controller think and hence the integrator works more causing overshoots. A possible solution to reduce this phenomena is to introduce a compensation, called $anti - windup$ technique, see Figure 3.

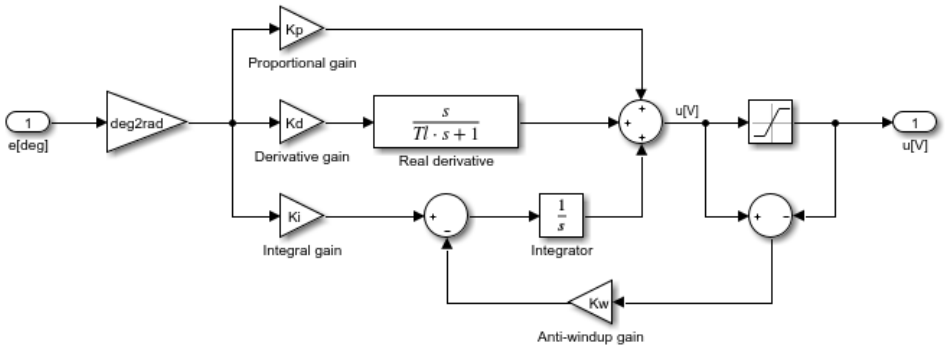

Figure 3: Block diagram of the PID controller with anit-windup mechanism

The continuous-time position PID controller for the DC servomotor which has transfer function:

$$C(s) = K_P + \frac{K_I}{s} + \frac{K_D s}{TLs + 1} \tag{5}$$

was designed using the Bode's design method (explained in the Section 3.2 of the Handout 0) using the plant transfer function (4) imposing $M\_p = 10\%$ and $t_{s;5\%} = 0.15$ s. The controller gains returned by this method are:

$$K_P = 8.6774 \quad K_I = 119.6293 \quad K_D = 0.1575 \quad T_L = 0.0059s \tag{6}$$

To evaluate the anti-windup gain, as a first trial consider to choose:

$$T_W = \frac{t_{s,5\%}}{5} = 0.03s \qquad K_W = \frac{1}{T_w} = 33.33 \tag{7}$$

In figure 4 it is evident that with the anti-windup compensator, the controller provides a better response, as it reduces the error in the integration caused by saturation of the controller, preventing excessive overshoots, mantaining the rise time performance and reduces a lot the settling time.

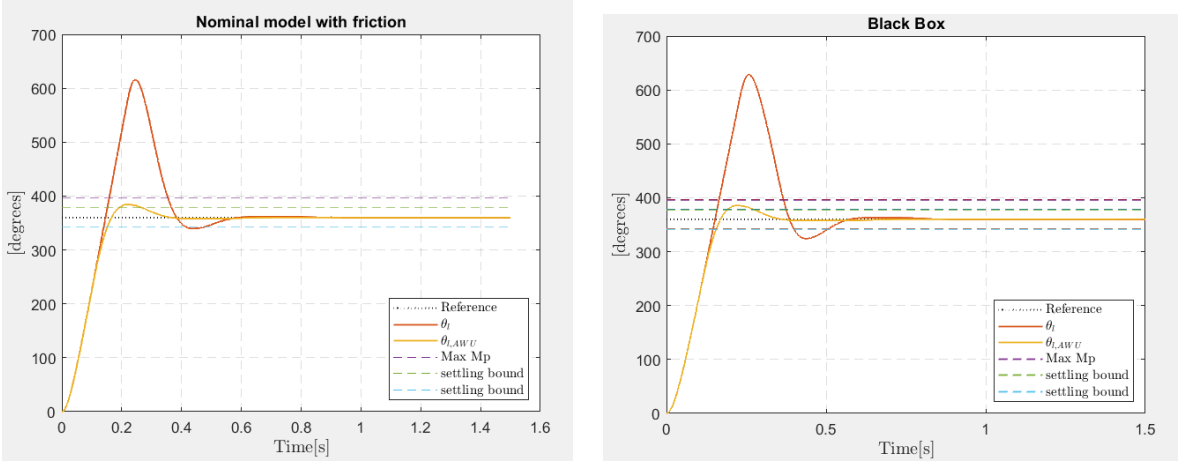

(a) (b)

Figure 4: Response of the closed-loop system to a 360deg step with and without anti-windup: Nominal model (a), real motor (b)

Thanks to the anti-windup mechanism, the transient now satisfies the requirement on M_P, decreasing the overhot from 71% to 6.7%, however, the constraints on the settling time are not respected, in fact the controller provides a settling time equal to 0.269s. In order to meet also this requirement specification on the step response, it has been necessary to adjust the PID parameters following a trial and error approach:

$$K_P = 7.9 \quad K_I = 119.6293 \quad K_D = 0.07 \quad T_L = 0.0059s \quad K_W = 66.66 \tag{8}$$

These gains lead to the step responses in figure 5, which respect all the constraints on the transient.

In table 1 you can see, in a schematic way, the comparison between all the model and the controller used.

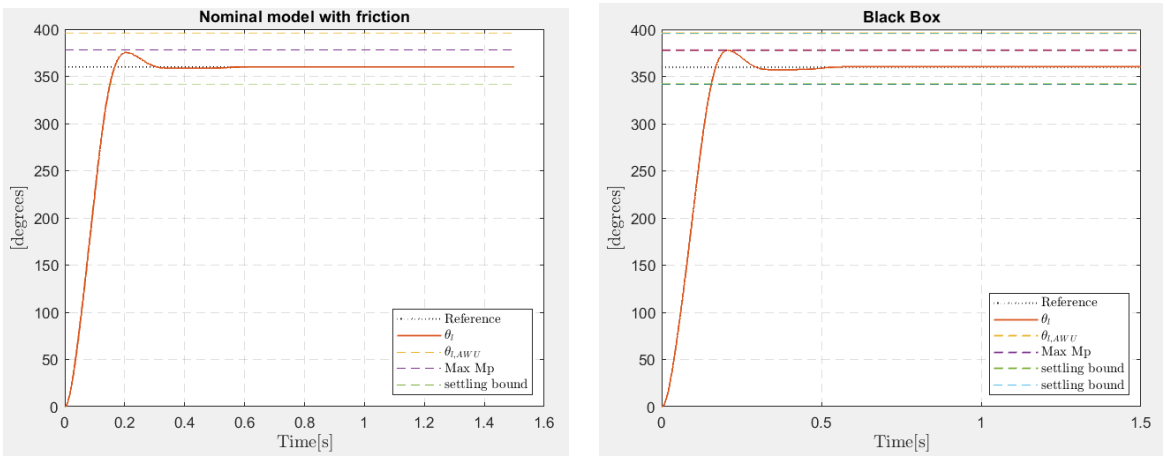

(a) (b)

Figure 5: Response of the closed-loop system to a 360deg step with and without anti-windup and the adjusted gains: Nominal model (a), real motor (b)

	$t_{s,5\%}[ms]$	$M_p[\%]$		$t_{s,5\%}[ms]$	$M_p[\%]$
Nominal	471	71	Nominal AWU	269	6.7
Real	506	74.55	Real AWU	274	7.1
Nominal adj.	486	77.5	Nominal adj. AWU	150	4.25
Real adj.	522.9	80.9	Real adj. AWU	152	5

Table 1: Result obtained by implementing the anti-windup mechanism. A green value means that such value meets the performance specifications

2.1.2 Feedforward compensation

A method used to reduce the controller's effort is to use a $feedforward$ compensation. This means use the knowledges of the plant, or the system to control, to design a nominal control that makes the output similar, even not exactly close, to the reference.
Now the feedback is used to compensate errors in the modelling procedure, or to increment the robustness of the control system.
The feed-forward scheme is showed in the Figure 3 of the Section 2.1 of the Handout 1, allows a compensation for the inertia, static and viscous friction and back-electromotive force.
The gains of the feed-forward circuit are reported in the following:

$$K_{IN} = 0.053, \quad K_{FR} = 48.2217, \quad K_{BEMF} = 0.1798 \tag{9}$$

For the test, a periodic acceleration reference signal with main period defined as follows, has been considered:

$$a_l^*(t) = \frac{d\omega_l^*(t)}{dt} = \begin{cases} 900rpm/s & \text{if 0s} \leqslant \text{t} < \text{0.5s} \\ 0rpm/s & \text{if 0.5s} \leqslant \text{t} < \text{1s} \\ -900rpm/s & \text{if 1s} \leqslant \text{t} < \text{2s} \\ 0rpm/s & \text{if 2s} \leqslant \text{t} < \text{2.5s} \\ -900rpm/s & \text{if 2.5s} \leqslant \text{t} < \text{3s} \end{cases} \tag{10}$$

which defines a trapezoidal speed profile. The speed and position references are obtained by integration of the acceleration profile, i.e.:

$$\omega_l^*(t) = \int_0^t a_l^*(\tau)d\tau \qquad \theta_l^*(t) = \int_0^t \omega_l^*(\tau)d\tau \tag{11}$$

The advantages brought by the direct chain compensation are clearly noticeable in the figure 6, where you can see that without feed-forward the absolute value of the tracking error exceeds 27degs, while with the feed-forward you have almost perfect tracking of the reference, with an absolute value of the error that does not exceed 1.75 deg.
In table 2 the result are riassumed in a compact way.

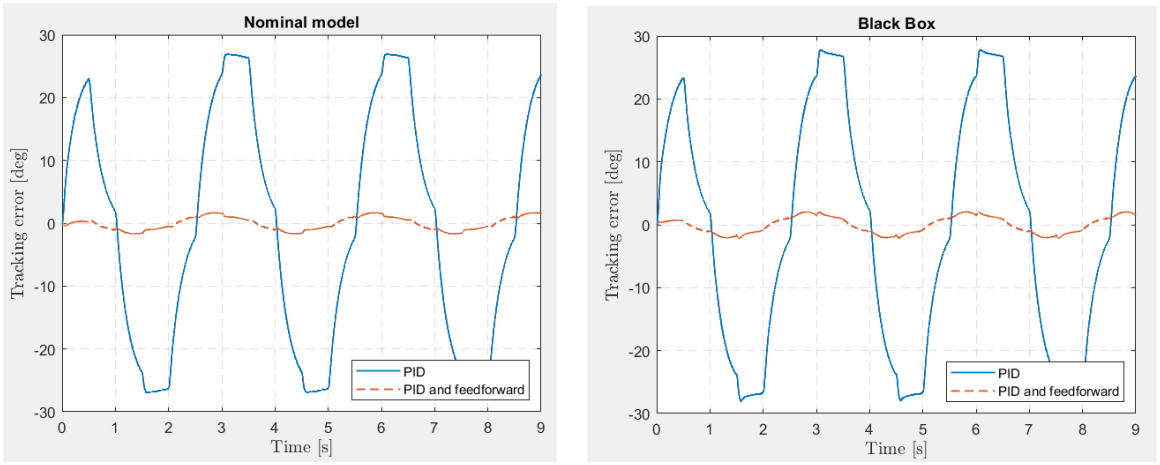

(a) (b)

Figure 6: Tracking error with and without the feed-forward mechanism: Nominal model (a), real motor (b)

	Nominal model		Real motor	
Feedforward	disabled	enabled	disabled	enabled
$\lvert e_{max} \rvert$ [degs]	27	1.75	28	2.23

Table 2: Tracking error comparison

2.2 State-Space Controller

2.2.1 Nominal tracking

The aim of this assigment is to design a state-space controller that guarantees the perfect tracking of constant position set–points in the nominal case.
The continuous-time position state-space controller in figure 7 was obtained by using the pole allocation method explained in the Section 3.2 of the Handout 1, using the state-space reachable and observable realization of the DC gearmotor transfer function (4):

$$A = \begin{bmatrix} 0 & 1 \\ 0 & -\frac{1}{T_m} \end{bmatrix} \qquad B = \begin{bmatrix} 0 \\ \frac{k_m}{NT_m} \end{bmatrix} \qquad C = \begin{bmatrix} 1 & 0 \end{bmatrix} \qquad D = 0 \tag{12}$$

In which the state is composed by the angular dispacement of the external gearbox and its rotation's speed: $x = [\theta_l \ \dot{\theta}_l]^T$.

The state and input feedforward gains are obtained by following the Handout procedure:

$$\begin{bmatrix} Nx \\ Nu \end{bmatrix} = \begin{bmatrix} A & B \\ C & D \end{bmatrix}^{-1} \cdot \begin{bmatrix} 0 \\ 1 \end{bmatrix} = \begin{bmatrix} 1 \\ 0 \\ \hline 0 \end{bmatrix} \tag{13}$$

Then, the control law becomes:

$$u = N_u r - K(x - N_x r) = -Kx + (N_u + KN_x)r \tag{14}$$

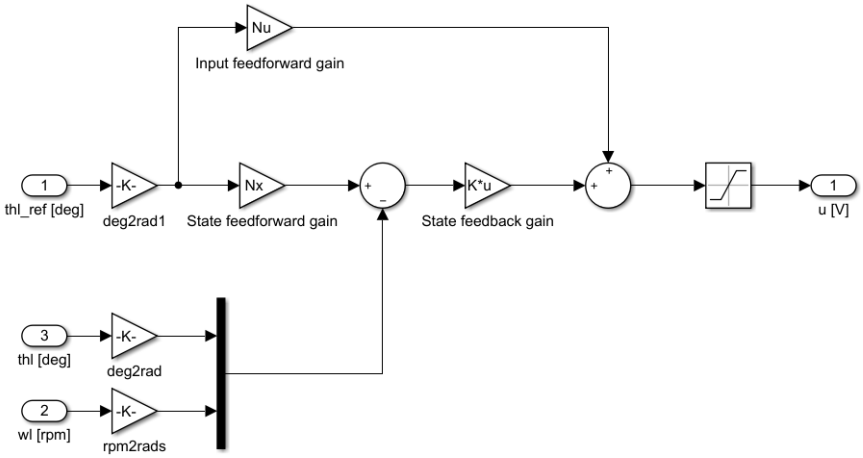

Figure 7: State space controller for nominal perfect tracking of constant set-points.

The assignment requires the following transient performances:

- nominal perfecct steady state tracking of step position (load side) references
- step response (load side) with settling time $t_{s,5\%} \leqslant 0.15s$ and overshoot $M_p \leqslant 10\%$

Resorting to the dominant pole approximation approach explained in Sec 3.1 of Handout 0, the eigenvalues of A-BK should be placed in:

$$\lambda_{1,2} = -\delta\omega_n \pm j\omega_n\sqrt{1-\delta^2} = -20 \pm j27.2875 \tag{15}$$

Where δ and ω_n are obtained by solving the following equations:

$$\delta = \frac{log(1/M_p)}{\sqrt{\pi^2 + log^2(1/M_p)}} \qquad \omega_n = \frac{3}{\delta t_{s,5\%}} \tag{16}$$

This dominant poles' allocation correspond to the state feedback gain K = [6.0907 0.0212].

Since the single output provide only one, the position, of the two components of the state necessary for the feedback, it is necessary to use a state observer. Instead of use a linear observer in state space, as it is common to do, a simplified observer has been used. This observer consists in a "real" derivarive, constructed through an high-pass filter, in order to obtain the velocity from the position, refer to figure 8 for the block scheme.

In figure (9) it is possible to see how effectively the nominal tracking works well for the ideal nominal model of the motor, i.e. considering all the frictions inside system equal to zero.
It is also evident that,instead, in the real nominal model of the motor the steady state error is not equal to zero, due to the fact that a non-null static friction is inside the motor model.
However, in the real system static friction is obviously present, in fact, performing the same

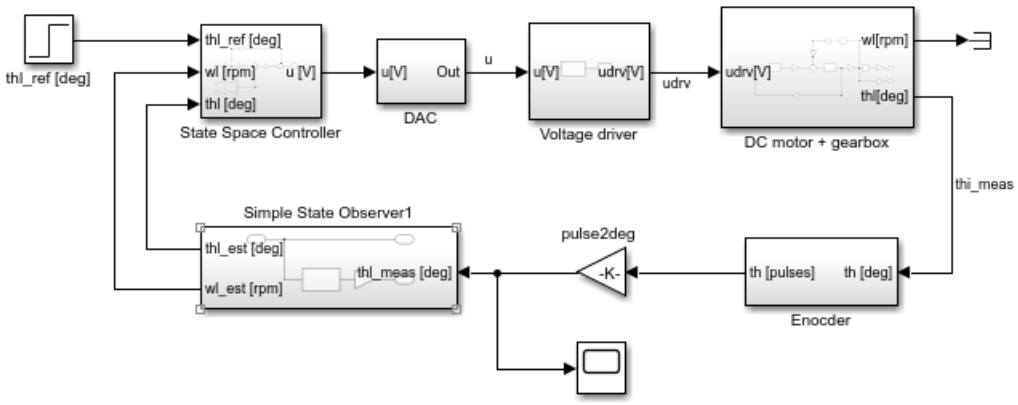

Figure 8: Block diagram of the system.

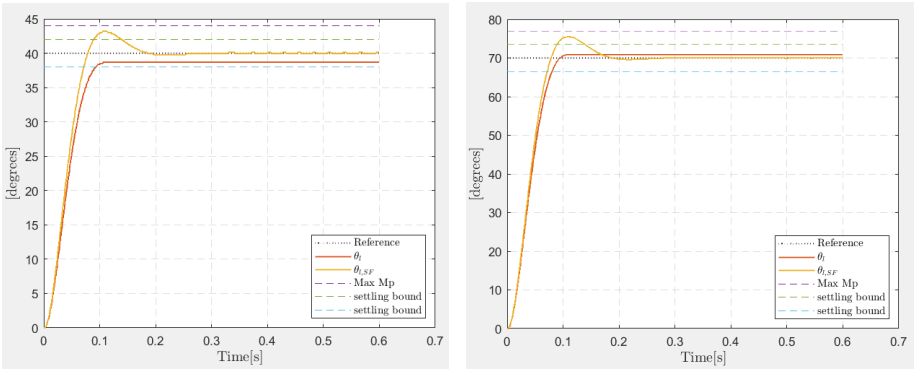

(a) (b)

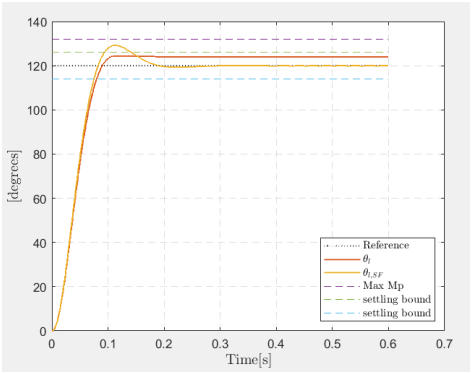

(c)

Figure 9: Step response of nominal model with and without the static friction: 40deg (a), 70deg (b), 120deg (c).

tests with the real motor, the results, figure 10, are very similar to the ones obtained in the nominal model considering the static friction as described above.

2.3 Robust tracking design with integral action

In order to guarantee perfect tracking of a constant reference input $r(t) = r_\infty \delta_{-1}(t)$ in presence of model uncertainties or constant disturbances entering at the plant input (such as friction), it is possible to introduce an integral action in the state-space controller in figure 7 .
The new state vector becomes $x_e = [x_I \;\; x]^T$, where x i the state vector of the previous

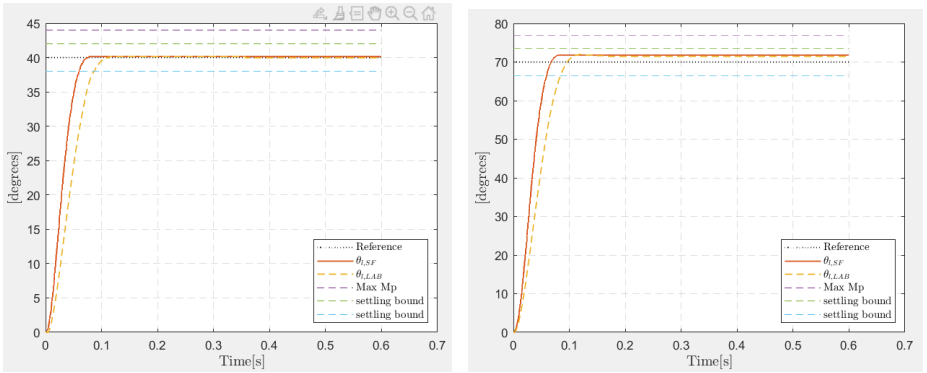

(a) (b)

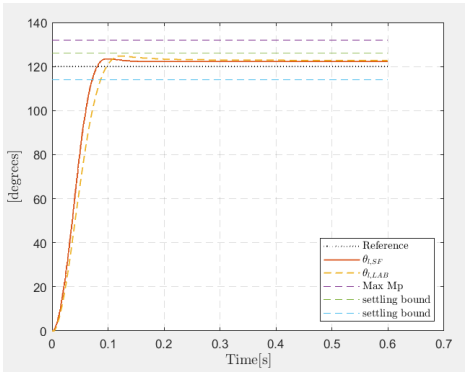

(c)

Figure 10: Step response of nominal model with static friction and the real motor in lab: 40deg (a), 70deg (b), 120deg (c).

assignment and x_I is the new added component.
Referring to the control law (14) the integral action can be included as follows:

$$u = -Kx + (N_u + KN_x)r - K_I \int_0^t [y(\tau) - r(\tau)]d\tau \tag{17}$$

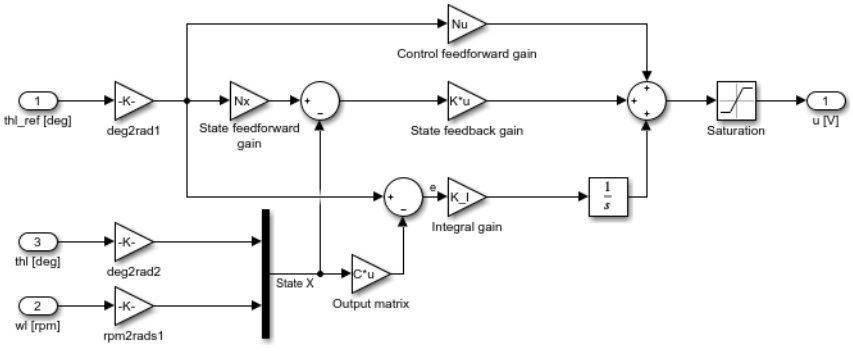

Figure 11: State space controller for nominal perfect tracking of constant set-points.

in which the integral component try to compensate the in some way the constant friction of the model or the modelling errors.
The feedforward matrixes N_x and N_u calculated in the previous point should remain un-

changed, but even so, you would have a very big overshoot that would ruin the performance specifications. The reason behind that behavior has to be researched in the position of the zeros in the closed loop transfer function, on which you do not have lot of control. A good solution is to decrease the value of N_x in order to decrease the overshoot's amplitude.
In figure 12 you can observe a comparison between the 70degs step response with the original N_x and the adjusted one N_x^*=$N_x/2$, that has been choosen in order to satify the spacifications on M_p.

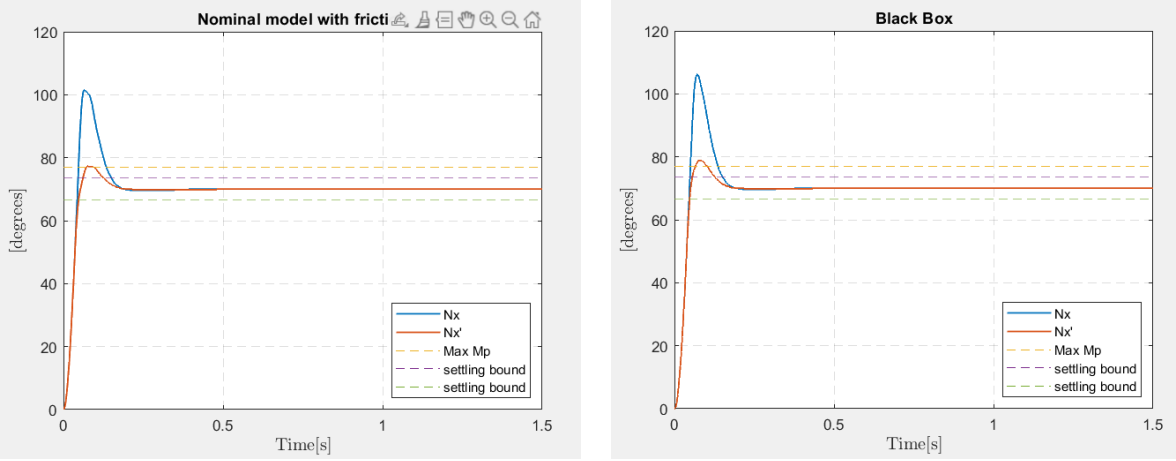

(a) (b)

Figure 12: Response to 70deg step whit N_x and N_x^*: Nominal model (a), real motor (b)

Note that reducing (modifying in general) N_x is not possible without the integral action, because in such a case only one value of N_u and N_x allows a perfect nominal tracking of step references.

The assignment proposed four choices for the eigenvalues:

- $\lambda_{c,\{1,2\}} = \sigma \pm j\omega_d \qquad \lambda_{c,3} = \sigma$
- $\lambda_{c,\{1,2,3\}} = 3\sigma$
- $\lambda_{c,\{1,2\}} = 2\sigma \pm j\omega_d \qquad \lambda_{c,3} = 2\sigma$
- $\lambda_{c\{1,2\}} = 2\sigma \pm j\omega_d \qquad \lambda_{c,3} = 3\sigma$

where σ and $\pm\omega_d$ are the real and imaginary parts of the eigenvalues in (15). These poles' locations imply the state-feedback gains, obtained following the Sec. 3.3 of Handout 1:

- $K_1 = [10.3476 \quad 0.1277] \qquad K_{I,1} = 121.8132$
- $K_2 = [6.3854 \quad 0.1277] \qquad K_{I,2} = 42.5693$
- $K_3 = [29.5038 \quad 0.4469] \qquad K_{I,3} = 499.0424$
- $K_4 = [38.0177 \quad 0.5533] \qquad K_{I,4} = 748.5636$

The choiche of the poles' location provide the step response in figure 13, in which it is possible to observe one of the differences between the previous point, in figure 9 for example, is that in this case the presence of the friction pratically does not influence the transient behaviour.

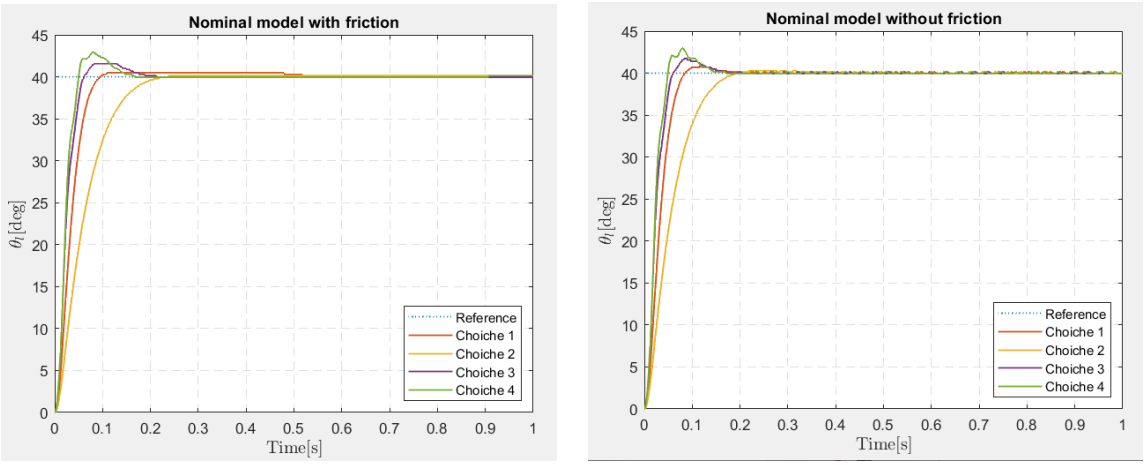

(a) (b)

Figure 13: Response to 40deg step whit different poles' location: Nominal model with static friction (a), nominal model without static friction (b)

Testing these different options with a 40deg step reference, it emerged that the best one is the third because its transient has the right speed/overshoot balancing, as shown in figure 13. With the chosen eigenvalues, and hence the chosen controller, the test has been performed with different amplitude of constant reference, see figures 14, 15 and 16.

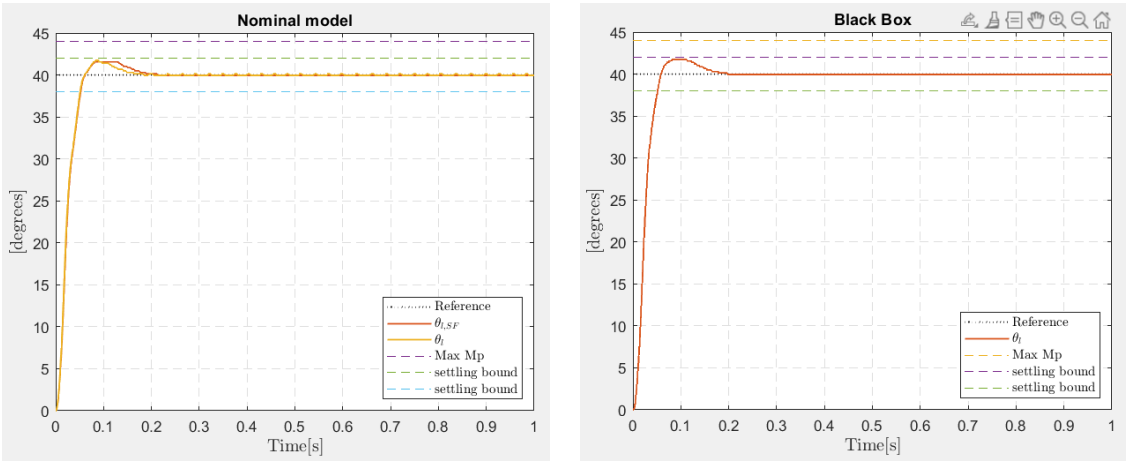

(a) (b)

Figure 14: Response of the closed loop system to 40deg with the third controller: Nominal model with and without static friction (a), real motor (b)

Clearly, the step responses in figure 16 greatly violate the constraint on the maximum overshoot, to solve the problem it would be sufficient to reduce again the value of Nx. In table 3 all the results are reported.

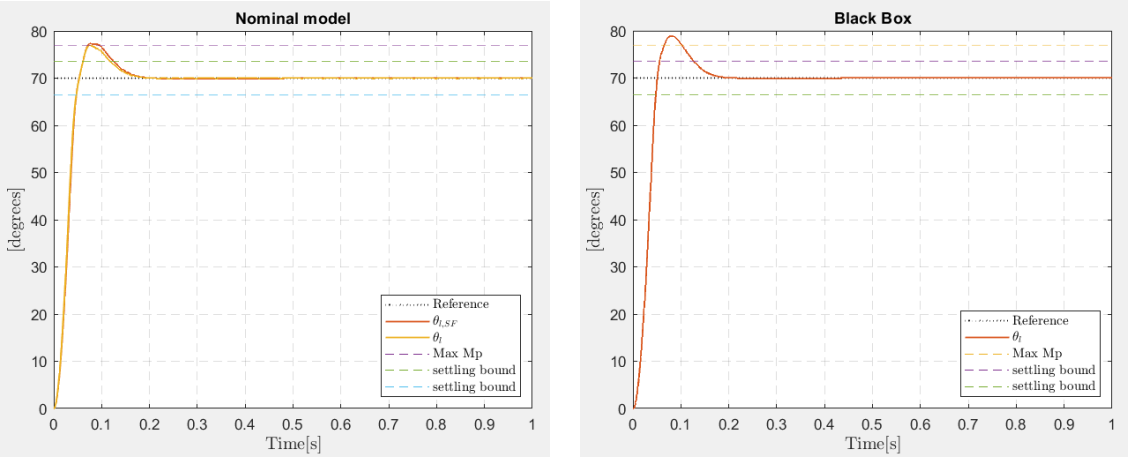

(a) (b)

Figure 15: Response of the closed loop system to 70deg with the third controller: Nominal model with and without static friction (a), real motor (b)

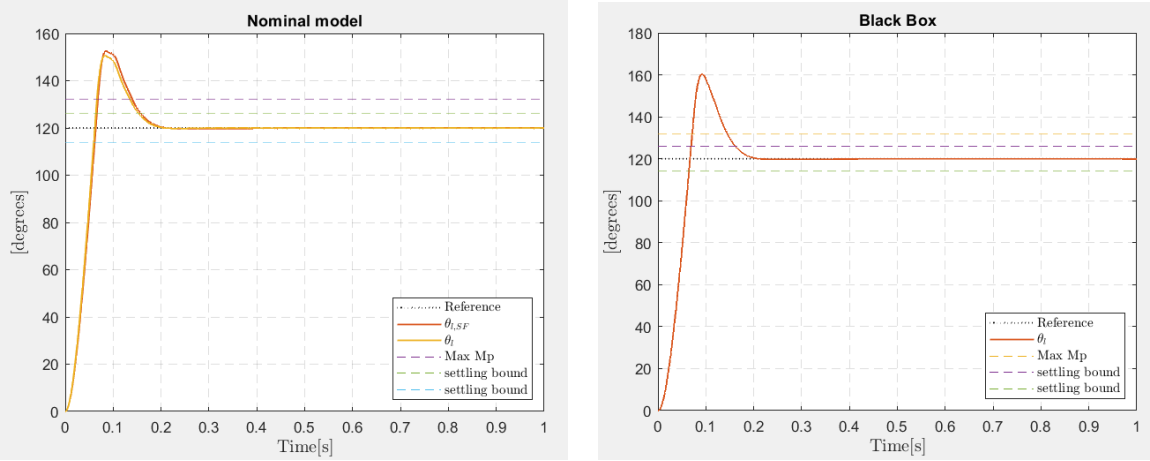

(a) (b)

Figure 16: Response of the closed loop system to 120deg with the third controller: Nominal model with and without static friction (a), real motor (b)

	40deg reference		70deg reference		120deg reference	
	$t_{s,5\%}$ [ms]	M_p [%]	$t_{s,5\%}$ [ms]	M_p [%]	$t_{s,5\%}$ [ms]	M_p [%]
Ideal Nominal	51.1	4.4	117.7	10.05	154	25.4
Real Nominal	52.1	3.95	117.7	10.57	158.5	27.05
Real motor.	51.9	4.4	125.7	12.63	161	33.65

Table 3: Result obtained by implementing integral controller in state space. A green value means that such value meets the performance specifications

2.4 Robust tracking design with error-space approach

To give to a control system the ability to track, with zero steady-state error, a more complex non decaying input and to reject a non decaying disturbance, such as ramp or sinusoidal input, there are many solutions. One of them is the so called, $error - space$ approach, which is based on including the equations satisfied by these external signals as part of the problem formulation.

This type of solution can be seen as a problem of regulation of the error, which is to say that the error $e(t)$ tends to zero as time gets large.
To solve the problem the reference $r(t)$ and the disturbance $w(t)$ are seen as solution of, in this case, second-order differential equations:

$$\ddot{r} + \alpha_1 \dot{r} + \alpha_2 r = 0 \qquad \ddot{w} + \gamma_1 \dot{w} + \gamma_2 w = 0 \tag{18}$$

In which, considering sinusoidal reference of frequency ω_0 and constant disturbance, (18) becomes:

$$\ddot{r} + \omega_0^2 r = 0 \qquad \dot{w} = 0 \tag{19}$$

Through the procedure explained in Sec. 3.4.2 of Handout 1 and considering the original system in (12), the following system is obtained:

$$\Sigma_z : \left[\begin{array}{c} e^{(1)} \\ e^{(2)} \\ e^{(3)} \\ \hline \dot{\xi} \end{array}\right] = \underbrace{\left[\begin{array}{ccc|c} 0 & 1 & 0 & 0 \\ 0 & 0 & 1 & 0 \\ 0 & -\omega_0^2 & 0 & C \\ \hline 0 & 0 & 0 & A \end{array}\right]}_{A_z} \underbrace{\left[\begin{array}{c} e \\ e^{(1)} \\ e^{(2)} \\ \hline \xi \end{array}\right]}_{z} + \underbrace{\left[\begin{array}{c} 0 \\ 0 \\ 0 \\ \hline B \end{array}\right]}_{B_z} u_\xi \tag{20}$$

In which ξ and u_ξ are respectively the error-space state and the error-space control:

$$\xi = \sum_i \alpha_i x^{(i)}(t) \qquad u_\xi = \sum_i \alpha_i u^{(i)}(t) \tag{21}$$

Looking at (20), it is possible to notice that the error component of the new state z is completely indipendent from the input and hence if Σ_z is asymptotically stable, with or without state-feedback control, the error and its derivatives converge to zero as t goes to $+\infty$.

The request is to do the design for the following choices of the period T_r of sinusoidal reference signal:

$$T_{r,1} = 0.15s \qquad T_{r,2} = 0.25s \qquad T_{r,3} = 0.5s \qquad T_{r,4} = 1s \tag{22}$$

consider the following tentative choice for the eigenvalues placement of $A_z - B_z K_z$:

$$\lambda_{c,\{1,2\}} = \omega_n e^{j(-\pi \pm \pi/4)} \qquad \lambda_{c,\{3,4\}} = \omega_n e^{j(-\pi \pm \pi/6)} \qquad \lambda_{c,5} = -\omega_n \tag{23}$$

where ω_n is the natural frequency of the dominant poles approximation in (16).
These poles' locations imply the following state-feedback controllers:

- $K_{z,1} = [2.3586 \cdot 10^5 \quad -3.5886 \cdot 10^4 \quad 2.5548 \cdot 10^2 \quad 36.9266 \quad 0.5548]$
- $K_{z,2} = [2.3586 \cdot 10^5 \quad 1.8061 \cdot 10^3 \quad 1.0937 \cdot 10^3 \quad 42.902 \quad 0.5548]$
- $K_{z,3} = [2.3586 \cdot 10^5 \quad 2.1732 \cdot 10^4 \quad 1.4473 \cdot 10^3 \quad 45.4229 \quad 0.5548]$

- $K_{z,4} = [2.3586 \cdot 10^5 \quad 2.7087 \cdot 10^4 \quad 1.5357 \cdot 10^3 \quad 46.0531 \quad 0.5548]$

To validate the previous design, the controller designed to track a sinusoidal reference input with period $T_r = T_{r,3} = 0.5s$, has been considered.The tests are performed with three different amplitudes of the sinusoidal signal (i.e. 30deg, 60deg and 90deg) .

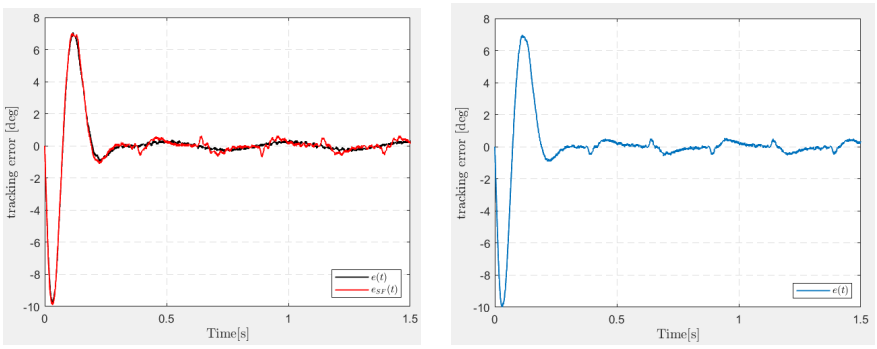

(a) (b)

Figure 17: Tracking errors with sinusoidal reference of amplitue 40deg and T_s=0.5: Nominal model with and without static friction (a), real motor (b).

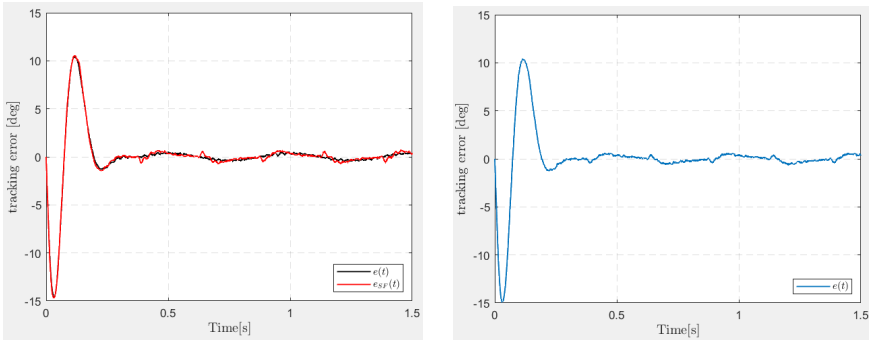

(a) (b)

Figure 18: Tracking errors with sinusoidal reference of amplitue 60deg and T_s=0.5: Nominal model with and without static friction (a), real motor (b).

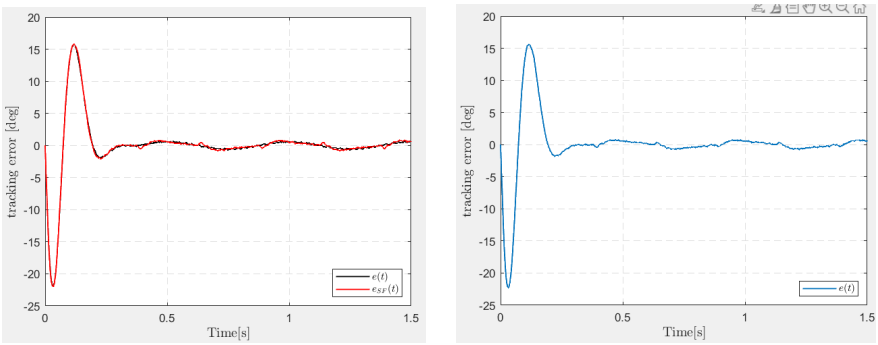

(a) (b)

Figure 19: Tracking errors with sinusoidal reference of amplitue 90deg and T_s=0.5: Nominal model with and without static friction (a), real motor (b).

Figures 17a,18a and 19a show that the tracking errors obtained in the real situation, considering the static friction, and the idela situation, neglecting static friction, present some

differences. In particular seems that the tracking error is slightly influenced by the presence of static friction.
This happens because the control system has been designed assuming a constant disturbance entering at the DC gearmotor input, but, as reported in Appendix **??**, static friction acts at the "Mechanical dynamics" block input.
If the disturbance would had been placed effectively at the plant input, the system would have been able to perfectly reject that constant disturbance.
A simple test can be represented by moving the static friction to the DC gearmotor input and analyse the tracking error in the real and in the ideal situation. From figure 20 it can be noticed that in this case the tracking error is not affected at all by the presence of the static friction.

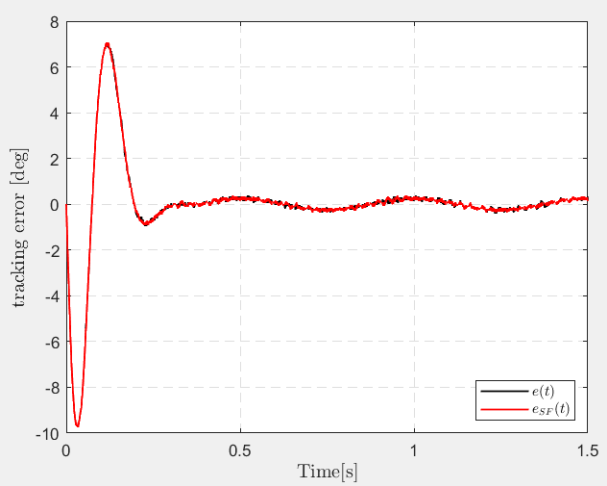

Figure 20: Tracking errors with sinusoidal reference of amplitue 40deg and T_s=0.5 changing the input's position of the static friction disturb.

Using the same controller evaluated at the previous point but varying the frequency of the sinusoidal input it is possible to see how the controller does not work correctly anymore. In fact the model of the new reference signal is not included in the controller and hence the system is not able to track the reference with zero steady state error.
As shown in figure 21, using the appropriate controller the tracking error goes to zero quite quickly, instead using the controller evaluated for another signal reference the tracking error does not go to zero at steady state.

Applying a step reference using the controller evaluated at previous point it is possible to notice that the output response follow quite well the reference. In theory the system should track with zero error the constant reference since the model of this reference is encapsulated in the the disturbance in (19). In practice it does not happen, have a look to figure 22.
It is interesting to observe, in figure 22b, that the perfect zero steady state tracking is obtained only with the ideal nominal motor model, in which the only error is probably due to a quantization error or limit cycles. The real motor model in simulation and the real motor in

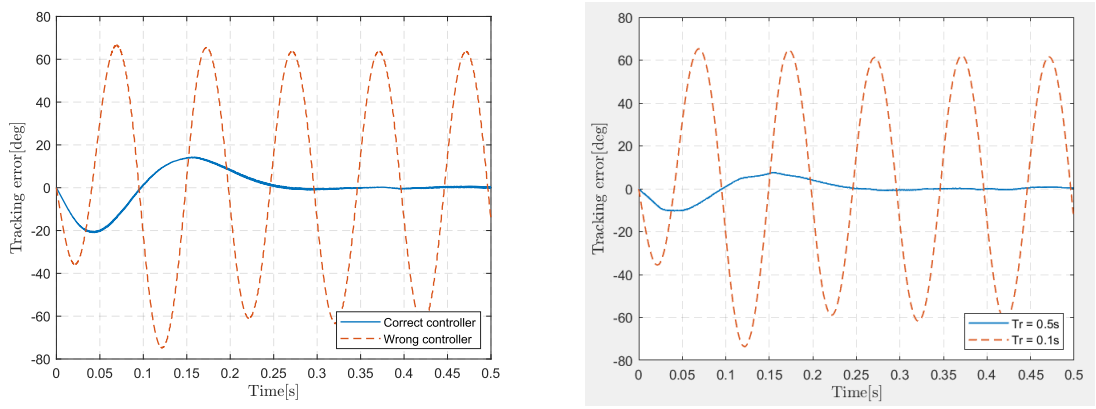

Figure 21: Simulation: Comparison of the error using the same controller, evaluated to track sinusoidal signal of period 0.5s, to track sinusoidal reference of period 0.5s and 0.1s: Nominal model (a), real motor (b)

laboratory experience provide a non-zero steady state error.
This is due, as in the previous case, by the fact that the constant disturbance enter at the "Mechanical dynamics" block input, instead of enter directly at the input of the whole system.

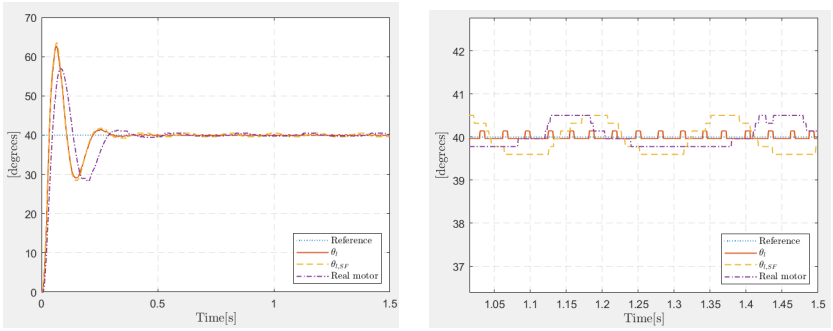

(a) (b)

Figure 22: Error state space tracking of constant reference in case of ideal/real simulation and with the real motor in lab experience: Full response (a), zoom at steady state (b)

2.5 Robust tracking design with extended estimator approach

Another way to solve the previous design problem is the so called $extended - estimator$ approach.
This method consists of estimating both the reference input and the load disturbance (i.e. disturbance entering at the plant input) with a state estimator,and then using the estimates to perform a reference plus disturbance feedforward compensation. The residual tracking error is finally driven to zero by designing a conventional state regulator.

For the design of the extended estimator, it is required to place the eigenvalues of the state-feedback section and the eigenvalues of the the extended state-estimator, consider the following

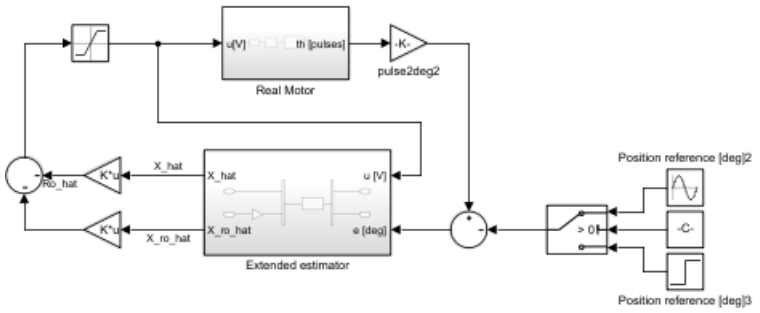

Figure 23: Block diagram of the extended estimator based controller.

tentative choice for the controller and estimator eigenvalues:

$$\lambda_{c\{1,2\}} = -\delta\omega_n \pm j\omega_n\sqrt{1-\delta^2} \tag{24}$$

$$\lambda_{e,\{1,2\}} = 2\omega_n e^{j(-\pi\pm\pi/3)} \qquad \lambda_{e,\{3,4\}} = 2\omega_n e^{j(-\pi\pm\pi/6)} \qquad \lambda_{e,5} = -2\omega_n \tag{25}$$

where ω_n is the natural frequency of the dominant poles approximation (**??**).
Then the following state-feedback controller has been obtained:

$$K = [6.0907 \qquad 0.0212] \tag{26}$$

Instead, considering always the choices of period T_r in (22), the following state-observer gain have been obtained:

- $L_{e,1} = [5.3511 \cdot 10^3 \quad -1.2250 \cdot 10^5 \quad -1.3578 \cdot 10^7 \quad 216.52 \quad 1.7851 \cdot 10^4]^T$
- $L_{e,2} = [9.8071 \cdot 10^3 \quad 3.1893 \cdot 10^5 \quad 1.3527 \cdot 10^6 \quad 216.52 \quad 2.1167 \cdot 10^4]^T$
- $L_{e,3} = [1.0444 \cdot 10^4 \quad 3.9155 \cdot 10^5 \quad 5.8982 \cdot 10^6 \quad 216.52 \quad 2.1652 \cdot 10^4]^T$
- $L_{e,4} = [1.0603 \cdot 10^4 \quad 4.1007 \cdot 10^5 \quad 7.1289 \cdot 10^6 \quad 216.52 \quad 2.1759 \cdot 10^4]^T$

To validate the design in simulation, the observer designed to track a sinusoidal reference input with period $T_r = T_{r,3} = 0.5s$, has been considered. It is interesting to notice that the poles' allocation of the estimator influences the evolution of the control. In fact, as shown in figure (24b), using an estimator with eigenvalues 4 times faster than those of A-BK the tracking error is quite smaller than the tracking error obtained an estimator with eigenvalues 2 times faster than those of A-BK.
This property could be explained saying thinking that more quickly the estimator is able to reconstruct the state, more quickly the state-feedback controller can drive the tracking error to zero. Instead if the estimator is more slow the estimation error goes to zero more slowly and hence the feedback controller works in a worst situation.

Analogously to assigment reguarding the error-space controller in Sec. 2.4, using the same controller evaluated at the previous point but varying the frequency of the sinusoidal input it

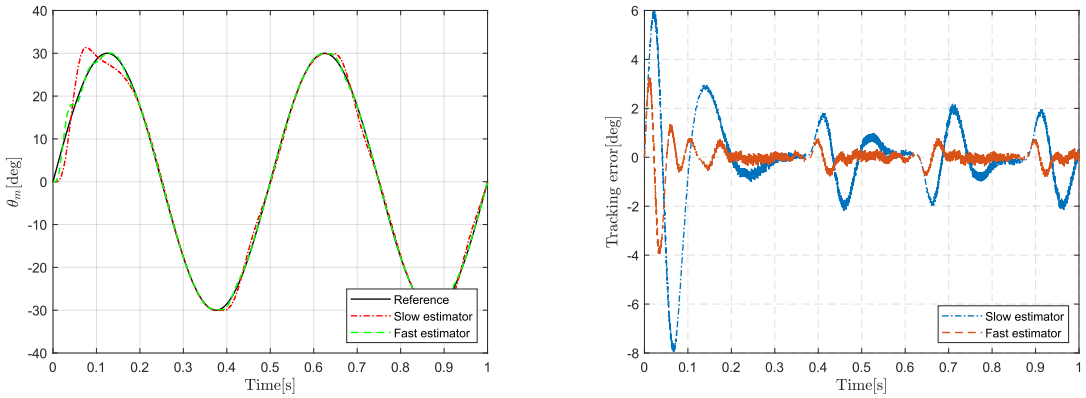

(a) (b)

Figure 24: Extended estimator tracking of of sinusoidal reference using two different extended estimators, one more fast than the other: Output response (a), tracking error (b)

is possible to see how the controller does not work correctly anymore. In fact the model of the new reference signal is not included in the controller and hence the system is not able to track the reference with zero steady state error .

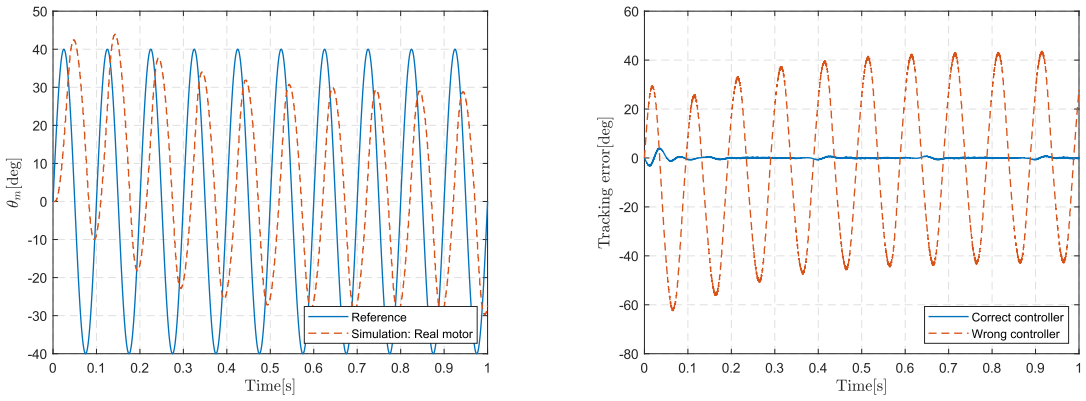

(a) (b)

Figure 25: Extended estimator tracking of sinusoidal signal: Output response using a controller evaluate to track sinusoidal signal of period 0.5s used to track sinusoidal reference of period 0.1s (a), comparison of the error using the same controller, evaluated to track sinusoidal signal of period 0.5s, to track sinusoidal reference of period 0.5s and 0.1s (b)

As shown in figure (25b), using the appropriate controller the tracking error goes to zero quite quickly, instead using the controller evaluated for another signal reference the tracking error does not go to zero at steady state.

A Appendix

A.1 Matlab code

A.2 Data sheet

A.3 Detailed calculations for PID design